doi:10.1093/brain/awt265 Brain 2013: 136; 3362–3377 | 3362

BRAIN
A JOURNAL OF NEUROLOGY

Use of quadrupedal step training to re-engage spinal interneuronal networks and improve locomotor function after spinal cord injury

Prithvi K. Shah,[1] Guillermo Garcia-Alias,[1] Jaehoon Choe,[2] Parag Gad,[3] Yury Gerasimenko,[1,4] Niranjala Tillakaratne,[1,5] Hui Zhong,[1] Roland R. Roy[1,5] and V. Reggie Edgerton[1,5,6,7]

1 Departments of Integrative Biology and Physiology, University of California, Los Angeles, California 90095, USA
2 Neuroscience, University of California, Los Angeles, California 90095, USA
3 Biomedical Engineering, University of California, Los Angeles, California 90095, USA
4 Pavlov Institute of Physiology, St. Petersburg, 199034, Russia
5 Brain Research Institute, University of California, Los Angeles, California 90095, USA
6 Neurobiology, University of California, Los Angeles, California 90095, USA
7 Neurosurgery, University of California, Los Angeles, California 90095, USA

Correspondence to: V. Reggie Edgerton, PhD,
Department of Integrative Biology and Physiology,
University of California,
Los Angeles,
610 Charles E. Young Drive,
Los Angeles,
CA 90095-1527,
USA
E-mail: vre@ucla.edu

Correspondence may also be addressed to: Prithvi K. Shah, PhD, E-mail: pshahucla@gmail.com

Can lower limb motor function be improved after a spinal cord lesion by re-engaging functional activity of the upper limbs? We addressed this issue by training the forelimbs in conjunction with the hindlimbs after a thoracic spinal cord hemisection in adult rats. The spinal circuitries were more excitable, and behavioural and electrophysiological analyses showed improved hindlimb function when the forelimbs were engaged simultaneously with the hindlimbs during treadmill step-training as opposed to training only the hindlimbs. Neuronal retrograde labelling demonstrated a greater number of propriospinal labelled neurons above and below the thoracic lesion site in quadrupedally versus bipedally trained rats. The results provide strong evidence that actively engaging the forelimbs improves hindlimb function and that one likely mechanism underlying these effects is the reorganization and re-engagement of rostrocaudal spinal interneuronal networks. For the first time, we provide evidence that the spinal interneuronal networks linking the forelimbs and hindlimbs are amenable to a rehabilitation training paradigm. Identification of this phenomenon provides a strong rationale for proceeding toward preclinical studies for determining whether training paradigms involving upper arm training in concert with lower extremity training can enhance locomotor recovery after neurological damage.

Keywords: spinal cord hemisection; rats; motor coordination; propriospinal system; quadrupedal locomotion

Received April 30, 2013. Revised August 26, 2013. Accepted September 1, 2013. Advance Access publication October 7, 2013

Introduction

Abundant anatomical and electrophysiological evidence demonstrates that spinal neuronal networks are exquisitely linked and modulated through ascending and descending propriospinal pathways (Jankowska *et al*., 1974; Juvin *et al*., 2005). Functionally, the propriospinal intersegmental linkage can mediate and/or facilitate motor coordination and regulate postural adjustments of the limb and trunk muscles during a variety of motor tasks in rodents (Juvin *et al*., 2005, 2012), cats (Jankowska *et al*., 2000; Gerasimenko *et al*., 2009), and humans (Dietz and Michel, 2009; Mezzarane *et al*., 2011). Descending propriospinal neurons receive input from the long descending supraspinal system (Kazennikov *et al*., 1991) as well as from direct afferent feedback from the limbs and trunk that can excite motor neuronal pools independently of supraspinal control (Akay *et al*., 2006). Furthermore, passive forelimb movements alone can facilitate hindlimb stepping in decerebrated cats through direct activation of propriospinal neurons (Gerasimenko *et al*., 2009). Additionally, several studies have demonstrated that the spared spinal pathways after a spinal cord injury undergo extensive reorganization to increase recruitment of propriospinal pathways for motor recovery, even in the absence of therapeutic interventions (Bareyre *et al*., 2004; Darlot *et al*., 2012). Collectively, these observations suggest that these interneuronal pathways could be used in rehabilitation paradigms by attempting to re-engage them after a severe spinal cord injury.

Activating interneuronal networks to enhance locomotor coordination has major implications for designing strategies that seek to use interlimb networks in gait rehabilitation after neurological injury (Behrman and Harkema, 2000; Ferris *et al*., 2006). There is some evidence showing that in individuals with spinal cord injury, rhythmic movements of the upper limbs enhance lower limb muscle recruitment during stepping (Visintin and Barbeau, 1994) or locomotor-like activity (Ferris *et al*., 2006; Kawashima *et al*., 2008). Clinical evidence demonstrating the direct impact of upper extremity training on lower extremity function, however, is preliminary and inconclusive (Behrman and Harkema, 2000; Tester *et al*., 2011). Moreover, animal studies using locomotor training paradigms to promote ipsilesional hindlimb locomotor recovery have not exploited the concept of actively 'training' the forelimbs (Battistuzzo *et al*., 2012).

We hypothesized that active involvement of the forelimbs through an intense quadrupedal step-training paradigm can facilitate the recovery of hindlimb function after a spinal cord injury. We demonstrate that training both the forelimbs and hindlimbs is more effective than training only the hindlimbs for the recovery of coordinated hindlimb function after a thoracic lateral hemisection in adult rats. We also hypothesized that the rostrocaudal interneuronal networks are re-engaged after quadrupedal training to enhance the locomotor recovery: this proposition is supported by the greater excitability of lumbar neuronal networks and greater neuronal labelling of propriospinal interneurons bilaterally above and below the lesion site.

Materials and methods

All experimental procedures were performed in compliance with the University of California Los Angeles Chancellor's Animal Research Committee and complied with the guidelines of the National Institutes of Health Guide for the Care and Use of Laboratory Animals (National Research Council, 2011).

Experimental groups, procedures and timeline

The experimental groups and timeline for the study are shown in Fig. 1. All surgeries were performed under aseptic conditions with the rats deeply anaesthetized with isoflurane gas (1.0 to 2.5%). The basic surgical procedures for the hemisection injury at T10 spinal segment and post-surgical care are as described previously (Shah *et al*., 2011). Forelimb (biceps brachii and triceps brachii) and hindlimb (tibialis anterior and medial gastrocnemius) muscles were implanted bilaterally with bipolar intramuscular EMG recording electrodes as described previously (Roy *et al*., 1991; Shah *et al*., 2011). Epidural electrodes were implanted at spinal cord segment S1 at the same time as the spinal cord hemisection (right side) surgery as described previously (Shah *et al*., 2012). To identify the propriospinal neurons, the retrograde tracer dye tetramethyl rhodamine dextran amine (TMD; molecular weight of 3000; 10% dissolved in distilled water, Invitrogen molecular probe D3308) was injected (by surgeons blinded to the study) below the hemisection into the right L2 segment of the spinal cord. Injections at L2 were chosen to target the long propriospinal terminal connections in the L2 intermediate grey matter that descend from the cervical enlargement at C5–C8 (Reed *et al*., 2006). Rhodamine tracer dye injections (four sites, 0.1 μl per site) were made stereotaxically into the right hemicord 0.67 mm lateral to the midline and at multiple depths starting at a depth of 1.2 mm and injecting every 0.3 mm while retracting towards the cord dorsum using a 100 μm glass micropipette mounted over a 10-μl Hamilton syringe. A total of 3 min was allowed between each injection. Two weeks after the tracer injections, the rats were anaesthetized deeply with sodium pentobarbital (450 mg/kg intraperitoneally), perfused transcardially with 150 ml of Sorenson's buffer solution containing sodium phosphate and NaOH, followed by 400 ml of 4% phosphate buffered paraformaldehyde, pH 7.4. The spinal cords were removed, post-fixed for 1–3 h, and stored in 30% sucrose in 0.1 M phosphate buffer.

Locomotor training

For quadrupedal step-training, the rats were placed on the treadmill surface to walk with full weight bearing on their forelimbs and hindlimbs. For the first 3–5 days of training, the trainer supported the rat's trunk to facilitate ground clearance of the right hindlimb during stepping. No such support was necessary thereafter. For bipedal step-training, an upper body harness was used to position the rats over the treadmill belt to enable bipedal locomotion (Shah *et al*., 2012). Rats were trained 7 days/week, at 21 cm/s, 35 min/session for ~2.5 weeks (total of 17 training sessions) starting 5 days after hemisection surgery. Animal groups randomly went through testing sessions on the first day and subsequent testing sessions were performed around the same time for each animal.

Kinematics and electrophysiological analyses of locomotor ability

Quadrupedal stepping ability on a treadmill at 21 cm/s was assessed before and 4, 8, and 21 days post-hemisection. Data were collected from 10–15 consecutive step cycles for the hindlimbs and forelimbs

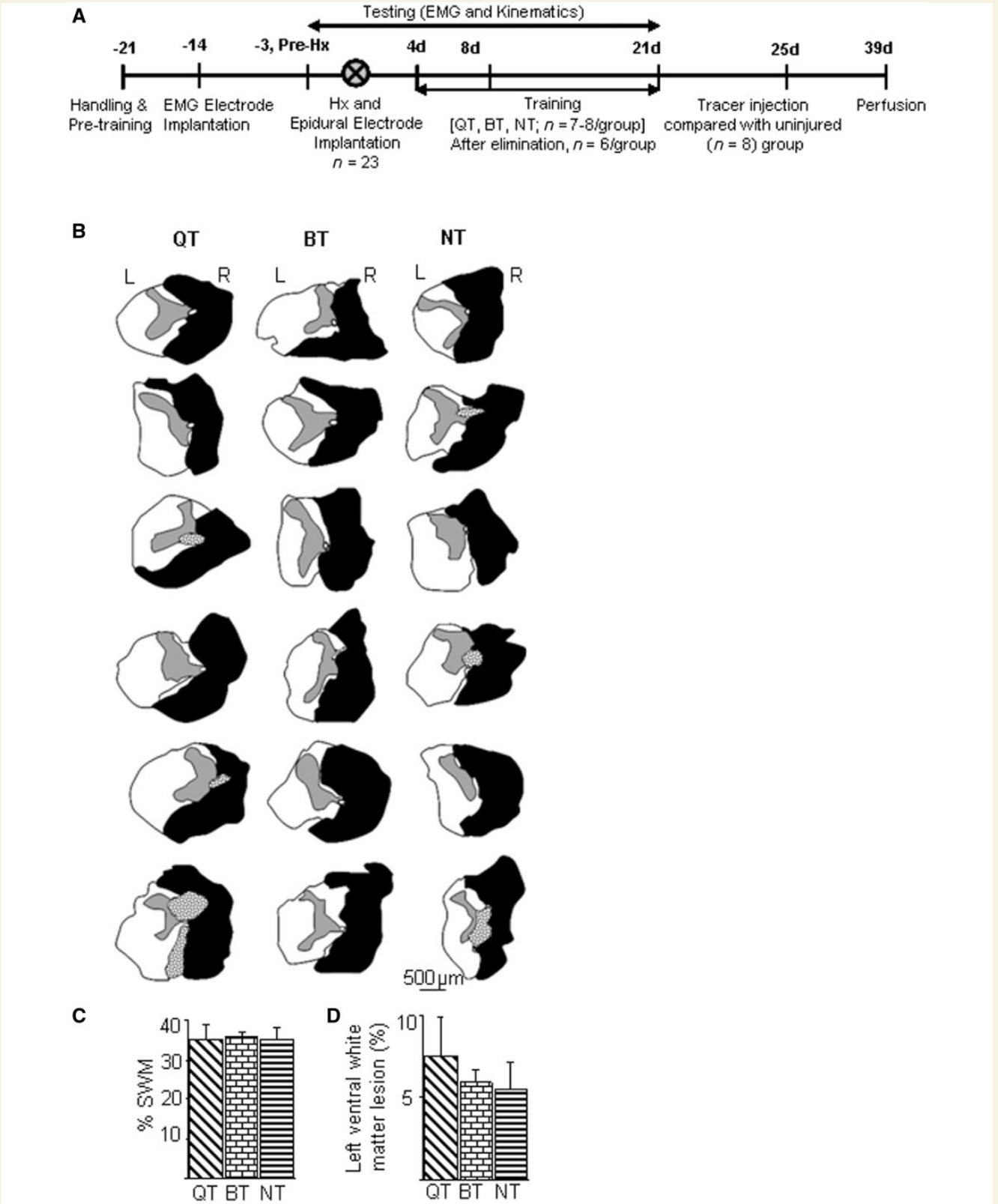

Figure 1 Timeline of experimental procedures and injury extent. (**A**) After initial handling and pretraining, rats ($n = 23$) underwent EMG electrode implantation in select forelimb and hindlimb muscles, implantation of spinal cord epidural electrodes, and a right lateral thoracic hemisection injury (Hx) at T10. Rats were either non-trained (NT, $n = 7$) or trained to step (30 min/day) quadrupedally (QT, $n = 8$) or bipedally (BT, $n = 8$) for 17 days beginning 4 days (4 d) post-hemisection. Data were collected pre-hemisection and at multiple time points post-hemisection. All accompanying data are presented from six animals per group after eliminating animals with an incomplete hemisection or dye diffusion. Retrograde tracers were injected into the spinal cord and the rats were later perfused. An uninjured group of rats

(continued)

bilaterally. EMG signals (2 kHz) were amplified and filtered (10–1000 Hz bandpass). Activation patterns (muscle waveforms and timing) for each muscle were obtained by taking an average of 10 filtered, rectified, and normalized (to the step cycle) EMG bursts from each muscle. Mean peak EMG amplitudes, integrals, and durations of identified EMG bursts from each muscle were computed for each rat during each testing session (Shah *et al*., 2012).

Kinematics data were collected using 3D video recordings. SIMI motion capture system (SIMI Reality Motion Systems) was used to obtain 3D coordinates of limb markers (at the iliac crest, hip, knee, ankle, metatarsophalangeal joint, and toe). A range of kinematics gait parameters including cycle period, stance phase duration, paw drag duration, and joint angle measurements were computed for each gait cycle. The quality of stepping and coordination within a limb (intralimb) and between the two hindlimbs and between the forelimbs and hindlimbs (interlimb) were assessed via both kinematics and electrophysiological measures as described below. Spatial consistencies of the hindlimb endpoint trajectories from the *x*–*y* coordinates of the ankle and metatarsophalangeal joint markers were measured as the amount of variance explained by the first principal component (Courtine *et al*., 2009). Placement of the foot on the treadmill during mid-stance, reflecting the vertical postural alignment and ability to support body weight at mid-stance, was measured as the vertical distance between the pelvis and knee joint markers and the treadmill surface.

At 21 days post-hemisection, epidurally-evoked motor responses were recorded during bipedal standing. An upper body harness was used to position the rats over the treadmill belt and the amount of body weight supported by the rat was maintained at 20% such that there was complete foot contact while the rat stood on the treadmill surface. Early and middle responses were evoked in the tibialis anterior muscles bilaterally via epidural stimulation (0.3 Hz, rectangular pulses, 0.5 ms duration, 10 kHz sampling frequency) at S1 (Lavrov *et al*., 2006) to determine the stimulus intensity-response amplitude curve. The responses of the tibialis anterior motor neuronal pool were measured as the peak-to-peak amplitude of averaged ($n = 10$ at each stimulation intensity) epidurally evoked potentials at stimulation intensities ranging from 0.5 to 5 V in increments of 0.5 V. Tibialis anterior middle responses were normalized to the mean maximum early responses recorded at the higher stimulation voltages (4, 4.5 and 5 V for each animal), as described previously (Lavrov *et al*., 2006).

Forelimb–hindlimb coordination

Forelimb–hindlimb coordination was assessed as the ratio of the number of forelimb steps for every 10 hindlimb steps before and post-hemisection. Forelimb/hindlimb ratios other than 1 indicate an uncoordinated gait. The mean horizontal distance between the right hindlimb and left forelimb and between the left hindlimb and right forelimb throughout a step cycle was computed for all steps analysed. Coordination between the forelimb and hindlimb was further quantified by computing the mean time lag between the contact of the toes on the treadmill surface for the right hindlimb and left forelimb and for the left hindlimb and right forelimb (Shah *et al*., 2012).

Inter-hindlimb coordination

Coordination between the two hindlimbs was determined kinematically by joint probability distribution plots obtained from the vertical (*y*) positions of the left and right metatarsophalangeal markers during 10 consecutive steps (Shah *et al*., 2012).

Intralimb coordination

To determine intralimb coordination, joint probability distribution plots were obtained from the rectified EMG activity of the tibialis anterior and medial gastrocnemius from the same hindlimb for 10 consecutive steps. A data point in these joint probability distribution plots represents the tibialis anterior and medial gastrocnemius activity in the same hindlimb at a given time in a single step and the overall pattern of data distribution qualitatively represents the intralimb coordination. Hip-knee and ankle-knee angle-angle kinematics plots were generated for the left and right hindlimbs to further examine intralimb coordination during stepping. The directionality of the plot trajectories was determined algebraically from differences in the vector-to-vector angle within specific phases of the step cycle and then the angles were summed to obtain the total change in angle for the trajectory (Fig. 6C and insets). The triangles described by angle-angle plots (Fig. 6C) were used to generate measures (see below) that were examined statistically to compare the shapes of each trajectory between steps, animals, and experimental groups (Fig. 6D). Maximum rotation of the shape trajectory was measured by comparing angles of segment AC with the *x* (hip) axis per step. Accordingly, a large anti-clockwise rotation of the trajectory results in large angles of segment AC that indicates a change in the angular phase relationships between joints within the hindlimb during stepping and hence reflects compromised intralimb coordination of the hindlimb.

Quantification of propriospinal neurons

Spinal cords were dissected, post-fixed in 4% paraformaldehyde for 1 h, and cryoprotected in 30% solution of phosphate-buffered (pH 7.4) sucrose at 4°C. Before sectioning, the cords were segmented into five blocks using the dorsal roots as landmarks as follows: C1–C5, C6–T1, T2–T6, T7–T10, T11–L1 and L2–L5. Spinal cord blocks were embedded in O.C.T. compound embedding medium (Tissue-Tek) in small peel-away histomolds, frozen over dry ice, and stored at −80°C until sectioning. Each block was cut transversely (30-μm thick sections), collected as free floating sections, serially mounted, and coverslipped with Vectashield® mounting media containing DAPI. A subset of sections adjacent to those used for tracer analysis was processed for immunofluorescent detection of the rhodamine tracer using an anti-rabbit tetramethylrhodamine antibody (Invitrogen).

The spinal cord sections were analysed using a rhodamine filter on a fluorescence microscope (Axio Imager 2, Carl Zeiss Microscopy, LLC). Digital images were captured using a camera and Image-Pro Plus

Figure 1 Continued
($n = 8$) was used for tracer dye injections out of which data from six animals are reported. (**B**) Histological reconstruction of spinal cord lesions: schematics of histological sections at the maximum extent of the spinal lesion (L = left; R = right) for six animals in the quadrupedal, bipedal, and non-trained groups show the extent of the hemisection lesion. Grey areas represent spinal grey matter, black areas scar tissue, and stippled areas cystic cavitations. (**C**) The spinal lesions quantified as the percentage of spared white matter (SWM) at the lesion epicentre normalized to intact white matter above the lesion site show no differences in the lesion areas among groups. (**D**) No differences were detected in the lesion extent of the contralateral (left) ventral white matter among groups.

software (Media Cybernetics Inc.). Spinal cord segmental levels were verified by the shape of the spinal cord matter and Rexed's laminae as a guide (Watson, 2009). The numbers of retrogradely labelled neurons were counted through the microscope eyepiece by a tester blind to the experimental design from every eighth section in each spinal block. Only neurons with a nucleus and proximal dendritic processes that were visible upon focusing up and down through the thickness of the section were included in the cell counts. Cell counts are reported from each spinal block as group means.

Assessment of hemisection lesion and dye injection site

The lesion size was determined by processing 30-μm spinal cord sections from segments T8–T11 using Cresyl Violet staining. The slides were dehydrated stepwise through alcohol, cleared in xylene, and cover-slipped with Permount (Fisher Scientific). The spinal cord sections were photographed and the lesion extent was quantified using ImageJ software (National Institutes of Health). Firstly, the total area of the white matter was measured in an uninjured rostral portion (~T8 spinal segment). The area of the white matter bridge at the lesion epicentre (the minimum white matter area) was measured and the ratio between these two measures ($\times 100$) was defined as the percentage of spared white matter for each animal. Secondly, the rostrocaudal extension (length) of the lesion was quantified as the distance between the most rostral and the most caudal transverse tissue sections in which evidence of tissue damage appeared with Cresyl Violet staining. Lastly, the area of contralateral ventral white matter lesion was quantified as a percentage of damaged ventral white matter at the lesion epicentre to the uninjured rostral white matter. Only the animals with a complete right spinal cord hemisection were included in the analyses (2 of 23 animals were excluded).

The area of tracer spread and dorsoventral and mediolateral spread of the dye (Fig. 7B) was determined from photomicrographs of the injection site and calibrated using a scale bar taken at the same magnification (Ballermann and Fouad, 2006). Animals in which the tracer injection site was not confined to the ipsilateral cord were excluded from further evaluation for histology ($n = 2$ for uninjured and 3 for the injured groups).

Statistical analyses

All data are reported as mean ± SEM. Overall significant differences were determined using one-way or two-way ANOVA or repeated measures ANOVA. Bonferroni *post hoc* tests were used to identify significant differences among individual groups. Normality of distribution was assessed by the Shapiro-Wilk test. Bootstrapping analyses (resampling model, 10 000 iterations with replacement) (Efron and Tibshirani, 1991) were used to determine statistical differences among groups for interlimb coordination. Differences among groups were considered statistically significant at $P < 0.05$. All statistical analyses were performed using MATLAB (Mathworks) and STATISTICA (Statsoft Inc).

Results

Spinal cord lesions

In all animals, complete lateral hemisection of the right hemicord was accompanied with minimal damage to the left ventral and dorsal white matter (Fig. 1B). The rostrocaudal extension of the hemisection (2.95 ± 0.08 mm in quadrupedal step-trained rats, 3.03 ± 0.11 mm in bipedal step-trained rats, and 2.76 ± 0.15 mm in non-trained rats), area of spared white matter (Fig. 1C), and lesion area of contralateral ventral white matter (Fig. 1D) did not differ among groups. Moreover, there was no correlation between the severity of injury and behavioural or electrophysiological outcomes in all animals.

Spontaneous motor recovery after a mid-thoracic lateral hemisection

Immediately after the thoracic hemisection, adult rats developed motor paralysis of the ipsilateral hindlimb that partially recovered during the first three weeks post-hemisection. Figure 2A–H shows detailed kinematics analyses of the right (lesioned side) forelimb and hindlimb of a non-trained rat before (pre-hemisection) and at 4, 8, and 21 days post-hemisection. Right hindlimb paralysis persisted for at least 4 days post-hemisection (Fig. 2B). Partial motor recovery was evident at 8 days post-hemisection: rats recovered some ability in the right hindlimb for weight support and some independent stepping (Fig. 2C). By 21 days post-hemisection, a gross pattern of normal locomotion was recovered, but all rats continued to show persistent motor deficits in the right hindlimb in stepping kinematics and most measures of stepping ability (see below and Supplementary Figs 1–4).

The kinematics and EMG data post-hemisection (Figs 2–6) demonstrate that the degree of locomotor recovery more closely resembled those recorded pre-hemisection (Supplementary Video 1) in rats that engaged both the forelimbs and hindlimbs (quadrupedal step-trained) than in rats that used only the hindlimbs during the treadmill training sessions (bipedal step-trained) or were not trained at all (non-trained, non-trained rats).

Quadrupedal step-training facilitates hindlimb stepping performance

After 17 sessions of training, quadrupedal step-trained rats had a shorter step cycle duration (Fig. 2I) and a lower per cent drag duration of the right hindlimb in a given step cycle (Fig. 2J) than bipedal step-trained rats and non-trained rats. Generally at 4 and 8 days post-hemisection, the forelimbs propelled the body forward by taking approximately twice the number of steps taken by the hindlimbs (Fig. 2B and C). This forelimb compensation had not returned to normal even at 21 days post-hemisection, although the forelimb-hindlimb step ratio was closer to pre-hemisection levels in quadrupedal step-trained rats compared with bipedal step-trained and non-trained rats (Fig. 2K). Quadrupedal step-trained rats showed a consistency in the ankle (Supplementary Fig. 2A) and toe (Supplementary Fig. 2B) trajectories similar to pre-hemisection animals, whereas these values in bipedal step-trained rats and non-trained rats were less consistent than in both the pre-hemisection and quadrupedal step-trained rats. The vertical postural trunk alignment of the body during stepping (as determined by knee and pelvis heights from the treadmill surface) showed similar values for pre-hemisection,

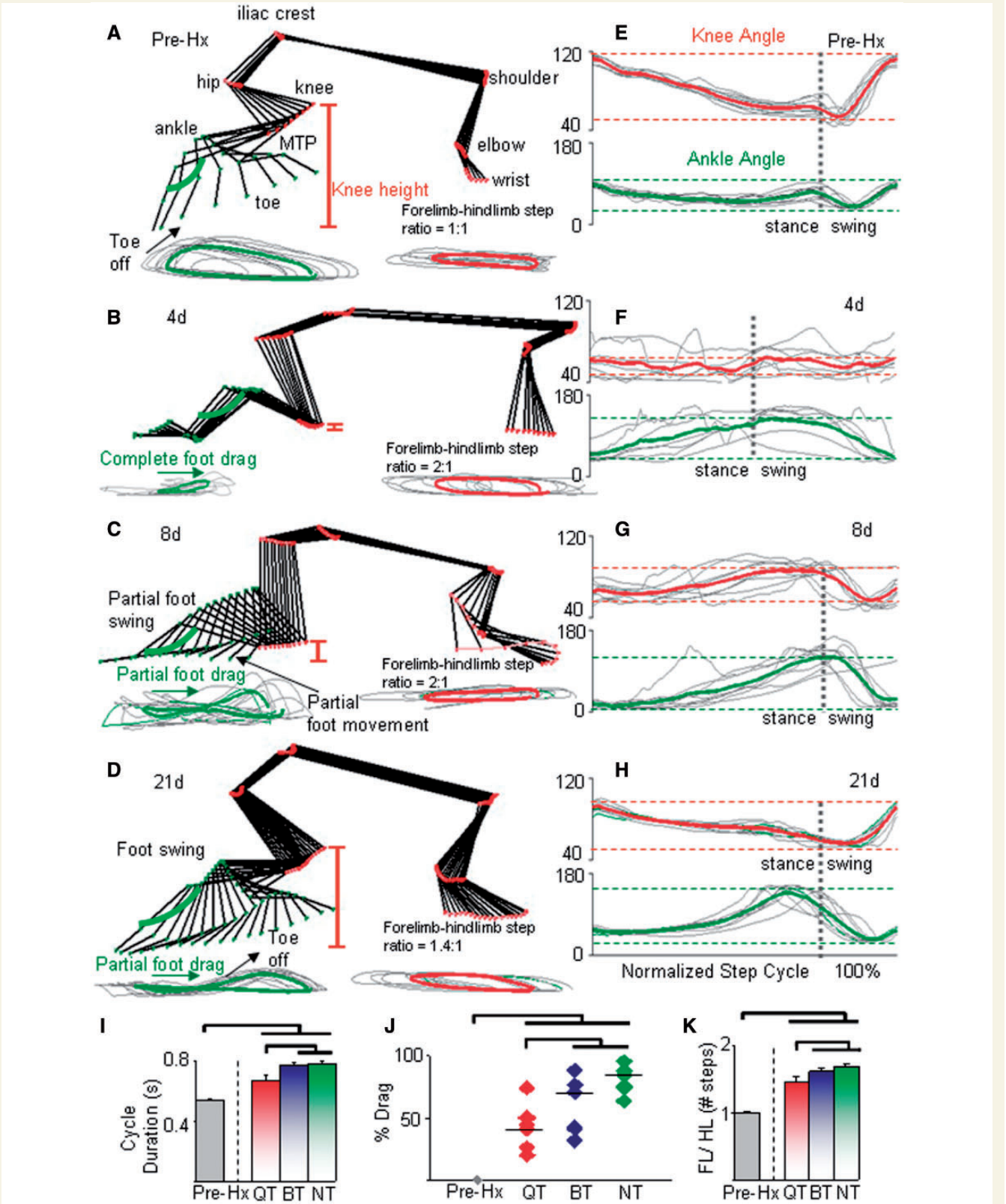

Figure 2 Spontaneous partial locomotor recovery post-hemisection (Hx). (**A–D**) Stick diagrams for a representative non-trained rat (NT) during the swing phase of a single step cycle for the right (lesion side) forelimb and hindlimb during quadrupedal stepping pre-hemisection (**A**) and at 4 (**B**), 8 (**C**), and 21 days (**D**) post-hemisection. Traces below the stick diagram show the foot (metatarsophalangeal (MTP) marker) and wrist joint trajectories for 10 consecutive steps (thin grey lines) and the corresponding mean values for the foot (thick green line) and wrist (thick red line). The red vertical lines indicate the vertical displacement of the knee from the treadmill (knee height). (**E–H**) Individual (thin grey lines) and mean knee (thick red line) and ankle (thick green line) angle movements for the same 10 steps as in **A–D**.

(continued)

quadrupedal step-trained and bipedal step-trained rats, but lower in non-trained rats (Supplementary Fig. 2C and D).

Quadrupedal step-training increases the recruitment and excitability of hindlimb motor neuronal pools

In the forelimb, there was a persistent increase in biceps brachii EMG activity bilaterally at 4, 8 and 21 days and a transient increase in triceps brachii EMG activity bilaterally at 4 and 8 days post-hemisection in all rats (data shown for non-trained rats in Fig. 3A), indicating compensatory forelimb activity propelling the body forward post-hemisection (Lopez-Dolado *et al*., 2013). Bilateral biceps brachii activity was decreased at 21 days compared with 8 days post-hemisection only in quadrupedal step-trained rats (Fig. 3B). Interestingly, the lower bilateral EMG activity in the biceps brachii in quadrupedal step-trained rats coincided with increases in bilateral hindlimb medial gastrocnemius EMG activity at 21 days compared with 8 days (Fig. 3D). These data suggest that there was greater recruitment of the hindlimb extensor motor neuronal pools during facilitated hindlimb stepping coincident with a decrease in forelimb flexor compensation with quadrupedal step-training. In contrast, tibialis anterior muscle activity remained largely unchanged in the right hindlimb at all time points in all rats post-hemisection, whereas there was an almost 2-fold increase in tibialis anterior activity in the left hindlimb of all groups at 21 days post-hemisection (Fig. 3D), irrespective of the training status. This elevated tibialis anterior activity persisted at 21 days post-hemisection most likely as a compensatory mechanism during the swing phase of the left hindlimb to support longer stance phase durations of the right hindlimb (Supplementary Fig. 1).

After quadrupedal step-training, epidurally evoked potential amplitudes in the tibialis anterior were similar bilaterally at each stimulation intensity tested 21 days post-hemisection, indicating similar excitability of the left and right tibialis anterior motor neuronal pools (Fig. 3E–G). In contrast, bipedal step-trained and non-trained rats showed higher amplitude responses in the right (lesioned side) versus left (non-lesioned side) tibialis anterior, indicating asymmetrical excitability. Interestingly, the threshold of epidural stimulation required to evoke a motor response (both early and middle responses) was lowest bilaterally after quadrupedal step-training, indicating overall greater excitability of the lumbosacral motor neurons (Fig. 3F–H). This could be because of changes in the intrinsic properties of the motor neurons. The ratio of the mean threshold of excitation for the early and middle responses was between 1–1.2 for all groups, indicating that the dorsally located axons (dorsal root fibres) could have evoked the middle responses.

Quadrupedal step-training improves interlimb and intralimb coordination during stepping

Forelimb–hindlimb coordination

The interlimb phase difference between the forelimb and diagonal hindlimb for consecutive steps was altered dramatically (Fig. 4A and B). Although a positive time lag was observed for the first two steps, a negative time lag persisted for the remaining eight steps during the test period at all time points in all rats, indicating that the hindlimb lagged behind the forelimb during consecutive steps in all groups (Fig. 4B). Accordingly, with larger time lags, there was less forelimb-hindlimb coordination. Quadrupedal step-trained rats had an ~80% decrease in time lags for the right hindlimb–left forelimb at 21 days compared with 8 days post-hemisection. Additionally, the horizontal distance between both forelimb-hindlimb combinations was longest at 4 days post-hemisection (Fig. 4C). Although this distance did not return to pre-hemisection values, step length distances between each forelimb-hindlimb combination was shortest in quadrupedal step-trained rats at 21 days post-hemisection (Fig. 4C), which enabled this group to step faster (Fig. 2I) and with greater consistency than bipedal step-trained and non-trained rats (Supplementary Fig. 2A and B).

Inter-hindlimb coordination

By 21 days post-hemisection, quadrupedal step-trained rats showed interlimb stepping coordination similar to pre-hemisection as reflected by: (i) the 'L-shaped' pattern in the joint probability distribution plots of vertical step heights for the right versus left hindlimbs (Fig. 5); and (ii) the time lag between the two hindlimbs (Supplementary Fig. 3A). Electrophysiological recordings also indicated greater reciprocity between hindlimbs in quadrupedal step-trained rats compared to the non-trained rats, but not bipedal step-trained rats (Supplementary Fig. 3B–D).

Figure 2 Continued
Dotted horizontal lines indicate the mean maximum and minimum joint angles at each joint and the dotted vertical lines indicate the transition between the stance and swing phases. Step cycle phases across groups are normalized to 100% of the step cycle. (**I**) Stepping at faster treadmill speeds in the quadrupedal step-trained rats (QT) than in the bipedal step-trained (BT) and non-trained rats at 21 days post-hemisection is indicated by shorter step cycle durations. (**J**) Mean percentage of foot drag during stepping is shorter in the quadrupedal step-trained rats than bipedal step-trained and non-trained rats. (**K**) The ratio of the number of forelimb steps for every 10 hindlimb steps (forelimb/hindlimb) is lower in the quadrupedal step-trained rats than in the bipedal step-trained and non-trained rats. Values are mean ± SEM for 10 steps for each group ($n = 6$/group). The first set of horizontal lines immediately above the bars indicate that the quadrupedal step-trained group is significantly different from the bipedal step-trained and non-trained groups; the second set of horizontal lines indicate significant differences between the pre- and each of the post-hemisection groups ($P < 0.05$). Similar convention is used in Figs 4 and 6 and in Supplementary Figs 2 and 3.

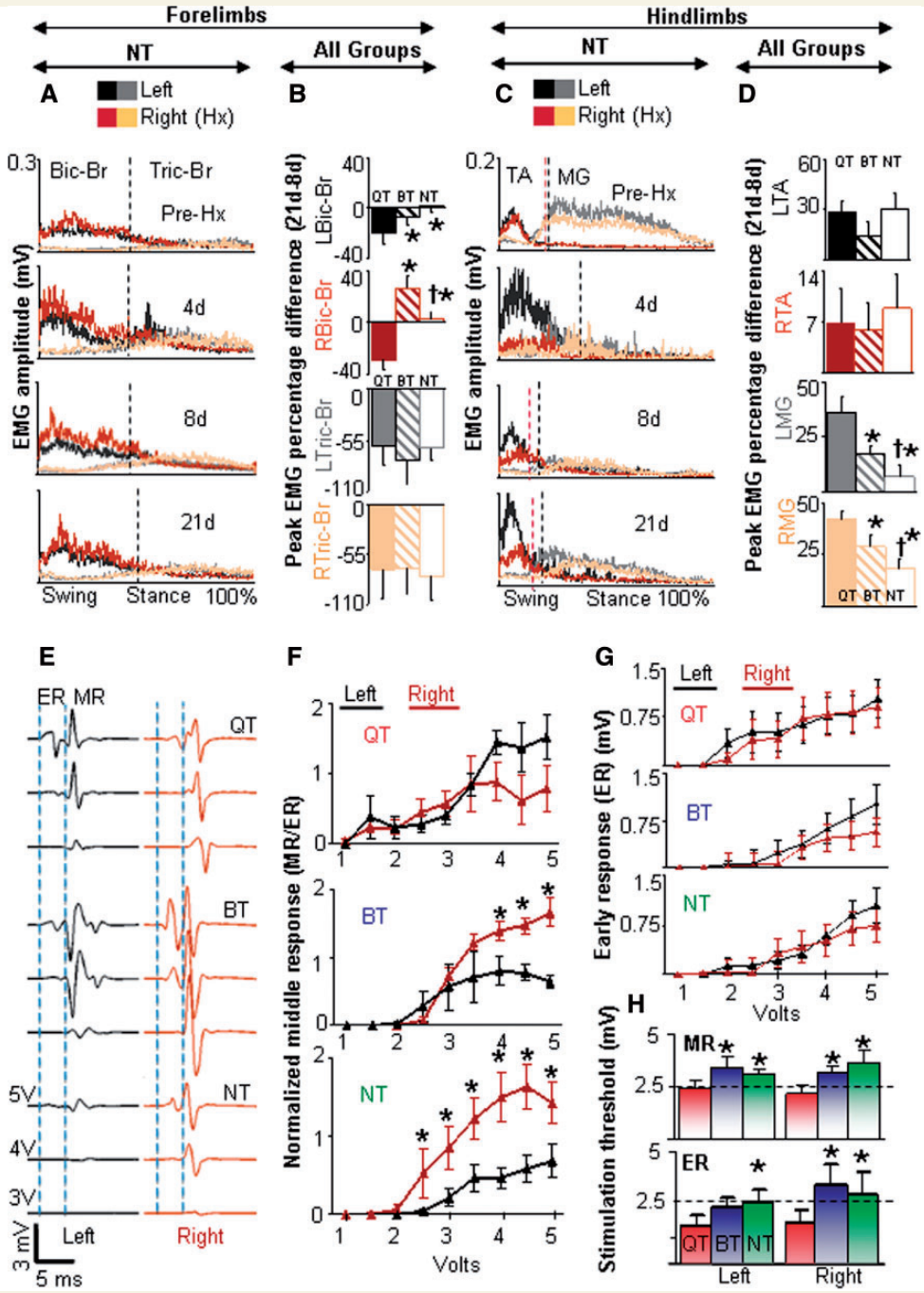

Figure 3 EMG recovery patterns post-hemisection and training. (**A**) Superimposed integrated rectified EMG activity patterns of the left and right biceps brachii (Bic-Br) and triceps brachii (Tric-Br) during quadrupedal stepping in non-trained (NT) rats ($n = 6$). This pattern of forelimb EMG activity was similar in all groups. Vertical lines indicate stance and swing phase durations that are normalized to 100% of the step cycle. (**B**) Percentage differences between 21 and 8 days (percentage difference 21days–8days) in the peak EMG amplitudes of the left (L) and right (R) biceps brachii and triceps brachii muscles demonstrate a maximum decrease in the peak amplitude of the biceps brachii muscle bilaterally in the quadrupedal step-trained rats (QT). (**C**) Superimposed integrated rectified EMG of the right and left tibialis anterior and medial gastrocnemius muscles for the same conditions as in (**A**). (**D**) Percentage differences between 21 and 8 days in the peak EMG amplitudes of the tibialis anterior and medial gastrocnemius muscles demonstrate a maximum increase in the peak amplitude of the medial gastrocnemius muscle bilaterally in the quadrupedal step-trained rats. *Significantly different from quadrupedal step-trained rats; †Significantly different from bipedal step-trained rats (BT) RMG = right medial gastrocnemius; LMG = left medial gastrocnemius; RTA = right tibialis anterior; LTA = left tibialis anterior. (**E**) Representative epidurally evoked responses from the left (black) and right (maroon) tibialis anterior in response to epidural stimulation for one rat per group at 21 days post-hemisection while standing and supported in a harness (20% body weight support). Vertical dashed lines identify the time periods for the early response (ER) and middle response (MR) in both the left and right tibialis anterior. The trace starts at the onset of the stimulation pulse. (**F**) Middle response amplitudes at various stimulation intensities from the left (black) and right (maroon) tibialis anterior normalized to the maximum early

(continued)

Intra-hindlimb coordination

An L-shaped pattern during stepping indicates a strong reciprocal activation between the tibialis anterior and medial gastrocnemius muscles (see pre-hemisection patterns in Figs 5 and 6A and B). At 21 days post-hemisection, an L-shaped pattern was most evident in quadrupedal step-trained rats. The amount of co-activation between the tibialis anterior and medial gastrocnemius muscles was highest in the right hindlimb (lesioned side) of non-trained rats (Fig. 6B). Importantly, there was no difference between pre-hemisection and quadrupedal step-trained rats bilaterally. But also in this instance, there was no significant difference between quadrupedal step-trained and bipedal step-trained rats. Qualitatively, the shape of the trajectory created by the joint angle plots was altered in all groups post-hemisection for hip-knee (Fig. 6D) and ankle-knee (Supplementary Fig. 4A and B) angles and maximum rotation of the trajectory for both hindlimbs was observed in bipedal step-trained and non-trained rats (Fig. 6D). Angle-angle plots also indicated that quadrupedal step-trained rats had angle-angle relationships not different from pre-hemisection, whereas bipedal step-trained and non-trained rats showed altered angle-angle relationships (Fig. 6E).

Quadrupedal step-training restores symmetry of gait kinematics

The difference in shape trajectories between the right and left hindlimbs was ~3° pre-hemisection, ~9° in the quadrupedal step-trained rats, and ~35° in the bipedal step-trained rats and non-trained rats, reflecting greater asymmetry in the angle-angle relationship between the two limbs during stepping in bipedal step-trained and non-trained rats (Fig. 6D and E). This change in shape trajectory and larger asymmetry in bipedal step-trained and non-trained rats results from a change in total hip joint excursion due to greater extension at the hip and lesser extension of the knee. The horizontal distance between the centroids of the shape trajectory of each hindlimb, an indication of asymmetry between the left/right hip and knee joint, was larger for bipedal step-trained and non-trained rats than quadrupedal step-trained and pre-hemisection rats (Fig. 6F).

Quadrupedal step-training promotes plasticity in the thoracic spinal interneuronal networks

We injected the retrograde tracer rhodamine red into the ipsilesional right L2 spinal segment and quantified the number of retrogradely labelled neurons in the cervical, thoracic, and lumbar spinal cord segments bilaterally (Fig. 7A). The tracer injection was confined mainly to the right dorsal and ventral grey matter of the L2 spinal segment (Fig. 7B and C). There were no differences in the dorsoventral and mediolateral spread of the tracer (Fig. 7B and C) or the area of the tracer spread at the site of injection (Supplementary Fig. 5) between groups.

In uninjured rats, retrogradely labelled neurons were visualized along the right and left grey matter of the entire spinal cord, including an even distribution along the segments of the cervical cord (Fig. 7D–F and L). In all injured rats, retrogradely labelled neurons were observed below and above the lesion in the right and left lumbar (Fig. 7G) and thoracic (Fig. 7H) segments. Nevertheless, no labelled cells were seen at the cervical segments in any group post-hemisection (Fig. 7I). Below the injury (T11–L1), quadrupedal step-trained rats had a greater number of retrogradely labelled propriospinal interneurons bilaterally than the non-injured, bipedal step-trained and non-trained rats (Fig. 7K). Above the hemisection (T8–T9), the number of labelled neurons bilaterally was lower in bipedal step-trained and non-trained rats than in the non-injured and quadrupedal step-trained rats (Fig. 7J). Cells were distributed throughout laminae V-VIII and X and along the medial border of the ventral horn. Few labelled cells also were located in laminae III and IV. The total numbers of neurons were similar in the left and right hemicord for each group with cell counts being highest in the lumbar and lowest in the thoracic segments (Fig. 7J and K). To examine the sensitivity of the rhodamine dextran-label, we counted the number of labelled cells using direct fluorescence and in sections processed for immunohistochemistry with anti-rabbit tetramethylrhodamine antibody (Invitrogen). There were no differences in the numbers of labelled cells detected by the two methods (data not shown).

Discussion

We hypothesized that actively involving the forelimbs would facilitate the recovery of locomotor function after a spinal cord injury. We demonstrate three novel findings: (i) actively engaging both the forelimbs and hindlimbs in a training paradigm (quadrupedal step-training) results in superior locomotor quality and coordination than training only the hindlimbs (bipedal step-training) or not training (non-trained); (ii) quadrupedal step-training is associated with greater excitability of motor neurons as is reflected in the lower levels of excitation thresholds of epidurally evoked potentials in the hindlimb muscles in both the lesioned and non-lesioned sides; and (iii) quadrupedal step-trained rats exhibit a significantly greater level of rostrocaudal thoracic interneuron connectivity as the they showed the highest number of labelled

Figure 3 Continued
response for each group. *Significant differences between the right and left hindlimb responses ($P < 0.05$). (**G**) Absolute early response amplitudes from the left (black) and right (maroon) tibialis anterior for each group. (**H**) Mean threshold of epidural stimulation to evoke a middle response and early response for the left and right tibialis anterior muscles for each group. Dotted black horizontal line indicates a threshold of 2.5 mV for the middle responses and early responses. *Significantly different from quadrupedal step-trained rats ($P < 0.05$). Values in **B**, **D**, **F**, **G** and **H** are mean ± SEM for six rats per group.

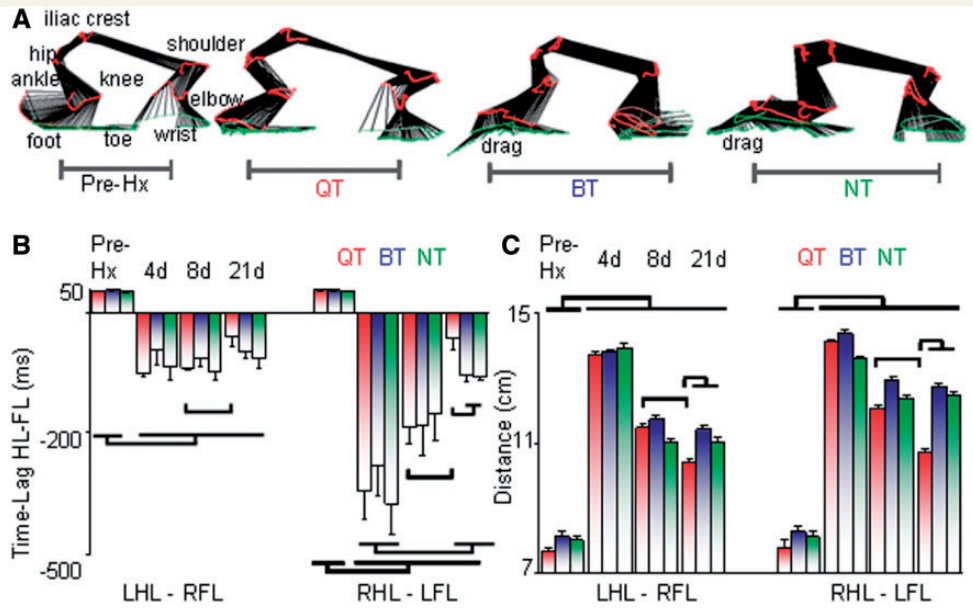

Figure 4 Quadrupedal step-training is effective in improving forelimb-hindlimb coordination. (**A**) Stick diagrams (30 ms between sticks) for a representative rat pre-hemisection (Pre-Hx) and from one rat per group at 21 days after a hemisection during the stance phase of a single step cycle illustrating the coordination patterns between the right hindlimb (RHL) and left forelimb (LFL) during quadrupedal stepping at 21 cm/s. (**B**) Bar graphs representing the lag times between the onset of the left hindlimb (LHL) and right forelimb (RFL) and between the right hindlimb and left forelimb contact on the treadmill during quadrupedal stepping at each time point. (**C**) Histograms depicting the horizontal distance between the left hindlimb and right forelimb and between the right hindlimb and left forelimb during quadrupedal stepping. After hemisection, the distance between the hindlimb and forelimb increases because of hindlimb drag, decrease in the knee height, and irregularities in the ratio of the number of forelimb steps for every 10 hindlimb steps (Fig. 2). Values in **B** and **C** are means ± SEM for ~10 steps/rat. Note that in **B** and **C** the quadrupedal step-trained (QT), bipedal step-trained (BT) and non-trained (NT) groups are significantly different from pre-hemisection at all time points and that the quadrupedal step-trained group is different at 21 days versus 8 days. Additionally, in both **B** and **C**, the quadrupedal step-trained group is different than both the bipedal step-trained and non-trained groups at 21 days.

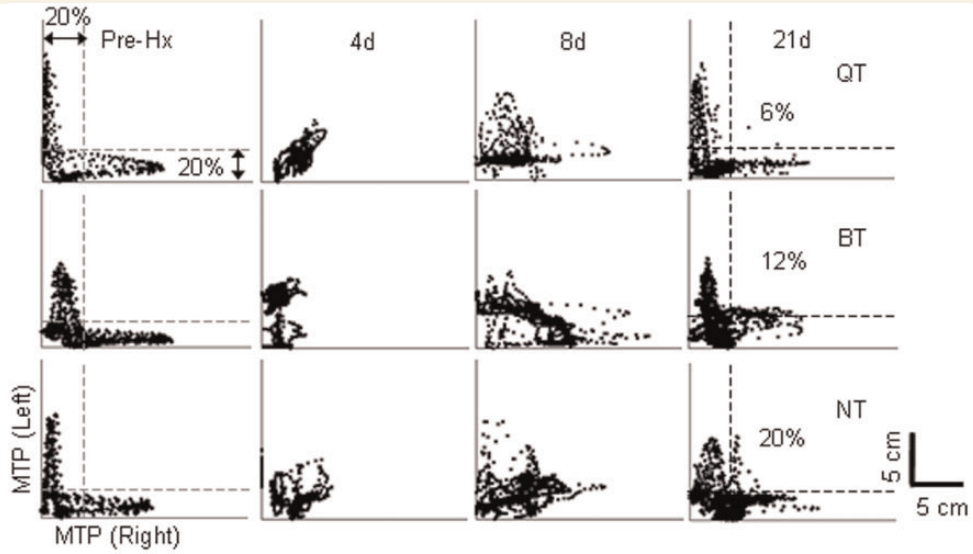

Figure 5 Quadrupedal step-training is effective in improving inter-hindlimb coordination. (**A**) Mean joint probability distributions of the *y* coordinates of the left and right metatarsophalangeal (MTP) markers during quadrupedal stepping before, and at 4, 8 and 21 days post-hemisection from all animals per group. An L-shaped pattern indicates an alternating motion of the two hindlimbs, whereas a D-shaped pattern indicates less alternation between the two hindlimbs. The percentage shown on the 21-day plots indicates the average number of data points that lie outside the 20% margins for an L-shaped pattern. Hx = hemisection; BT = bipedal step-training; QT = quadruped step-training; NT = non-trained.

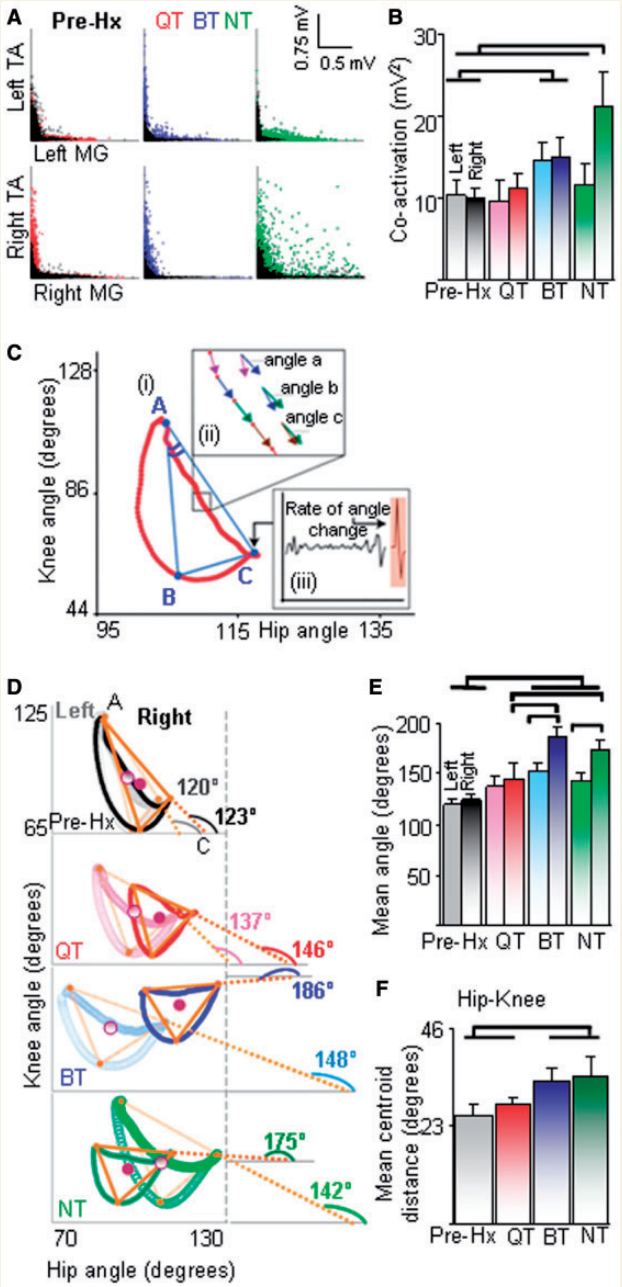

Figure 6 Quadrupedal step-training (QT) improves intralimb coordination and limb symmetry. (**A**) Joint probability distributions of rectified EMG for the tibialis anterior (TA) and medial gastrocnemius (MG) within each hindlimb during quadrupedal stepping pre-hemisection (Hx) (superimposed black dots) and 21 days (coloured dots) post-hemisection. (**B**) The levels of tibialis anterior and medial gastrocnemius co-activation within each limb are similar after quadrupedal and bipedal step-training (BT) and highest in the right hindlimb of the non-trained (NT) rats. (**C**) A triangle is prescribed from the angle-angle plots. Angle A of the trajectory (**i**) indicates the relationship between the knee and hip joint angles during the transition from swing to stance, segment AC represents this relationship during stance, and segments AB and BC during swing. Angle C of the trajectory represents transition from stance to the swing phase. Angle B of the trajectory represents transition between the initial and middle portions of the swing phase. For both stance and swing, propriospinal neurons above and below the hemisection site bilaterally.

Forelimb training in the recovery of hindlimb function

To test the hypothesis that actively engaging the forelimbs can promote locomotor function, we employed a simple, yet intense quadrupedal step-training regimen (21 cm/s, 30 min/session for 17 sessions). Training of the forelimbs in this manner served as a condition in which the full set of afferent and efferent inputs/outputs during quadrupedal locomotion were used. Compared with bipedal step-training, quadrupedal step-training includes the use of the forelimbs during treadmill walking and involves natural biomechanical adjustments of the entire body for proper control of posture and locomotion (Perennou, 2012). To isolate the effects produced by forelimb training, a sub-group of animals underwent bipedal hindlimb step-training. Assuming that supraspinal influences were similar in all the groups, we attributed differences in motor recovery between the quadrupedal and bipedal step-trained rats to the use of the forelimbs.

To our knowledge, no studies have determined the impact of functionally engaging the forelimbs to improve coordinated quadrupedal locomotion or have emphasized the effects of engaging the propriospinal pathways connecting cervico-thoraco-lumbar networks to promote recovery after a spinal cord injury. Although human studies show that upper extremity activity can acutely influence lower extremity motor function (Visintin and Barbeau, 1994; Huang and Ferris, 2004), none have clearly demonstrated whether chronically engaging the upper limbs in training facilitates lower limb function. Studies report that the

Figure 6 Continued
the trajectory is converted into sequential vectors (**ii**, inset) and the changes in vector-vector angles (example angle b – angle a) that indicate consistency between joint angles in each phase of the step cycle are computed algebraically. An example of the change in angle from the stance to swing phase (rate of change of angle at point C) is indicated by the angle trace (filled orange) in inset (**iii**). (**D**) Intralimb coordination determined kinematically via angle-angle plots illustrates the mean right (dark trace) and left (light trace) hindlimb knee-hip angle trajectories from a representative animal in each group. The orange triangle is an algebraic representation of the trajectory shapes as explained in **C**. The angle of segment AC with the hip joint axis was utilized to indicate the shape of the trajectory. Maximum anti-clockwise rotation of the right hindlimb shape trajectory reflects a change in angular phase relationships between joints within the hindlimb during stepping. (**E**) Asymmetry between the two hindlimbs is indicated by the differences in the angle prescribed by segment AC with the hip angle axis between the right and left hindlimbs and by (**F**) greater distances between the centres of trajectories between the right and left hindlimbs (centroid of triangles, maroon circles in **D**). Values in **A**, **B**, **E** and **F** are mean (±SEM) for 10 steps from all animals per group and the horizontal lines above the bars indicate significant differences between and among groups ($P < 0.05$).

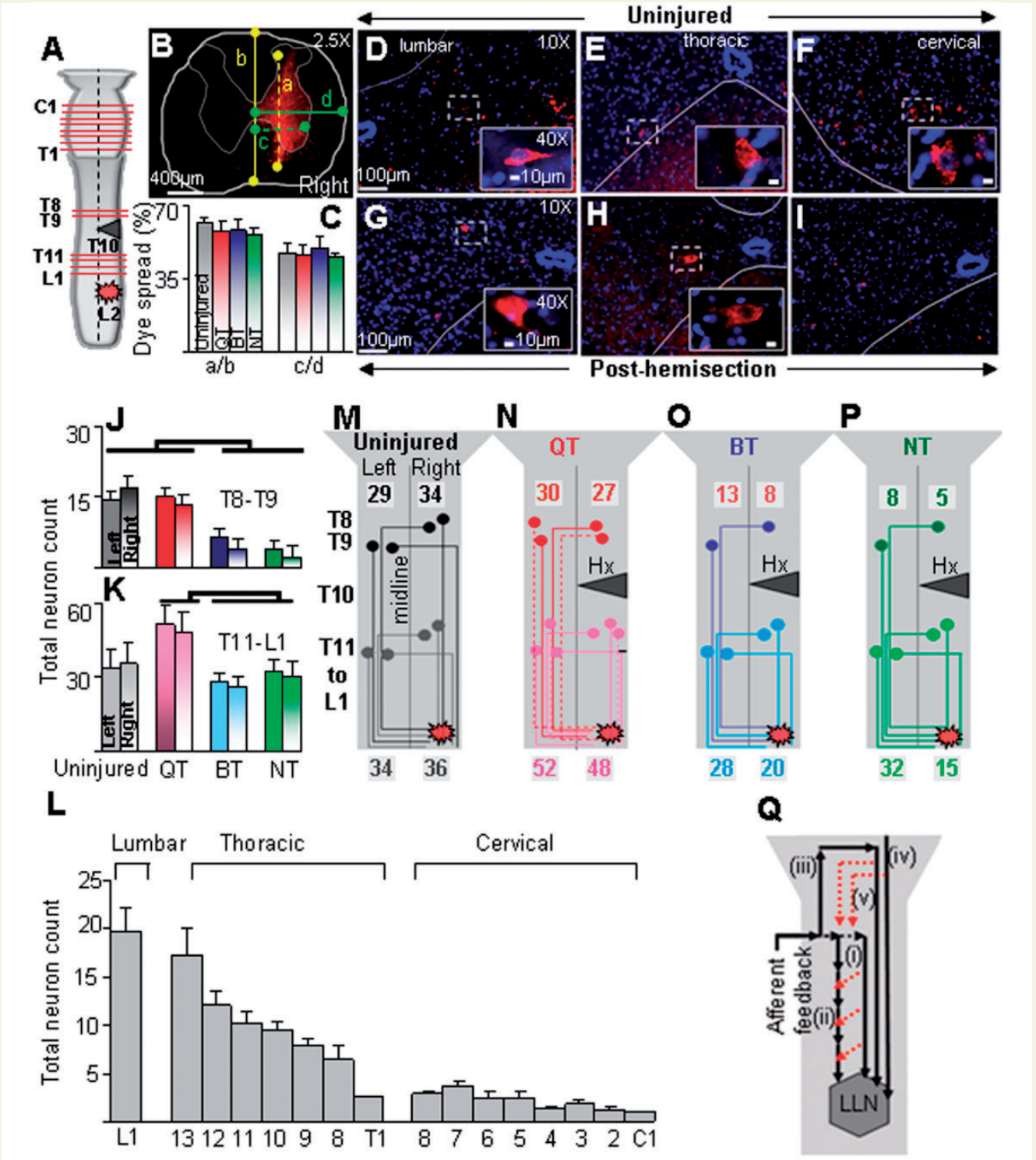

Figure 7 Quadrupedal step-training (QT) is associated with greater neuronal reorganization. (**A**) Schematic illustrating the hemisection at T10, sites of dye injection at L2, and cross sections where labelled cell counts were made. (**B**) Localization of rhodamine tracer dye at injection site in a representative animal shows that the dye was confined to the ipsilateral hemicord. The dorsoventral (yellow dotted) spread of the dye was normalized to the dorsoventral depth (solid yellow) of the cord (a/b) and the mediolateral spread of the dye (green dotted) was normalized to the mediolateral width (solid green) of the hemicord (c/d). (**C**) Both dorsolateral (a/b) and mediolateral (c/d) spread of the dye were uniform among the groups. Representative transverse micrographs of lumbar (**D**), thoracic (**E**), and cervical (**F**) spinal cord segments show retrograde-labelled neurons in an uninjured rat. Neuronal labelling is seen in all rats 39 days post-hemisection at the lumbar (**G**) and mid-thoracic (**H**), but not the cervical (**I**), spinal cord segments. Mean (±SEM) neuronal counts in the left and right hemicords above (T8–T9; **J**) and below (T11-L1; K) the hemisection. (**L**) Histograms showing the mean (±SEM, $n = 6$) total number of labelled cells in select lumbar, thoracic, and cervical spinal segments in uninjured animals. The number of labelled cells was

(continued)

magnitude of leg muscle recruitment during recumbent stepping and cycling increases as healthy subjects push against elevated mechanical resistance with their arms (Huang and Ferris, 2004) or perform higher frequencies of rhythmic arm cycling (Ferris *et al*., 2006; Hundza and Zehr, 2009). Similarly, in individuals with an incomplete spinal cord injury, there is some facilitation of the lower extremity muscles in spinal cord injury subjects when walking with, versus without, the arms swinging (Visintin and Barbeau, 1994; Behrman and Harkema, 2000). This facilitation was phase dependent on the step cycle (Kawashima *et al*., 2008). Interlimb coupling of upper extremity movements and stimulation of the peripheral nerves in the upper extremities also can modulate reflexes in the legs (Mezzarane *et al*., 2011). Whereas all of the abovementioned reports demonstrate that sensory input from the arms can contribute to the modulation of the motor output from the legs in humans, we show that actively engaging the forelimbs by 'training' over a period of 2.5 weeks elevates the EMG activity in the hindlimb muscles and enhances spinal cord excitability resulting in a significant improvement in locomotor function after spinal cord injury in rats.

Role of afferent input from the forelimbs

We propose that the ensemble of afferent input from the forelimbs during quadrupedal stepping strongly influences the neural substrates that impact coordination between the forelimbs and hindlimbs as well as between the two hindlimbs. It is well established that afferent volleys from the forelimbs induced by electrical stimulation of the brachial plexus or mechanical stimulation of the forepaw evokes direct responses of flexor and extensor lumbosacral motor neurons (Aoki and McIntyre, 1975; Schomburg and Steffens, 1986). In humans, interlimb coupling between the arms and legs is strengthened by adding cutaneous feedback from the hand during a normal locomotor rhythmic activity of all four limbs (Zehr *et al*., 2007). In the present study, bipedal step-trained and quadrupedal step-trained rats were able to step at similar treadmill speeds, but the 'added' afferent input from the forelimbs and trunk most likely was associated with the enhanced locomotor function observed with quadrupedal training.

The additional effects on locomotor recovery observed with quadrupedal step-training are attributable to one or more of at least three mechanisms [Fig. 7Q(i–iii)]. First, afferent feedback from the forelimbs can influence hindlimb activity through the direct activation of the long descending propriospinal pathways (Akay *et al*., 2006; Gerasimenko *et al*., 2009). Second, the forelimb to hindlimb interactions could be a consequence of chains of several inter-connecting short propriospinal axons (Aoki and McIntyre, 1975; Kostyuk and Vasilenko, 1979; Cowley *et al*., 2008). Third, afferent feedback from the forelimbs could be conveyed by ascending supraspinal pathways to locomotor regions in the brainstem or cortical structures from which the bulbospinal pathways descend. This spino-bulbo-spinal loop is activated by afferent input from the forelimbs that ultimately projects onto the spinal cord (Kausz, 1986) and may contribute to the prominent lumbosacral motor neuron discharge evoked by forelimb stimulation (Shimamura *et al*., 1967). Below, we discuss the role of the propriospinal system as one of the mechanisms of locomotor recovery.

Role of the propriospinal system in the recovery of locomotion

The long propriospinal neurons in the cervical spinal cord of the rat project ipsilaterally and contralaterally to the lumbar cord with the majority of the crossings taking place in the cervical or lumbar enlargement (Reed *et al*., 2006). Given their extensive remodelling capacity (Iannotti *et al*., 2003; Bareyre *et al*., 2004), robust capability to respond to therapeutic interventions (Houle *et al*., 2006; Deng *et al*., 2013), and their role in interlimb coordination (Zehr and Duysens, 2004) after spinal cord injury, we expected to detect retrotraced neurons in the cervical spinal cord of quadrupedal step-trained animals after a unilateral tracer dye injection below the thoracic lesion site. Surprisingly, we did not observe any propriospinal neurons in the cervical enlargement in all groups post-hemisection. A reduction in the amount of dye transport in the long propriospinal cervical neurons has been reported after thoracic spinal cord contusion injury in rats (Conta and Stelzner, 2004, 2010). Thus, the absence of cervical labelled neurons in our study could be attributed to: (i) the nature of the injury, i.e. compared with a lateral hemisection, contusion injuries preserve bilateral ventral and ventro-lateral white matter through which a majority of the propriospinal system descends (Reed *et al*., 2006, 2009); or (ii) the relatively lower volume of tracer dye injected in the present study. It must be noted, however, that the volume injected was adequate to observe retrotraced dyes in the cervical spinal cord of our uninjured animals (Fig. 7L) and low enough to prevent dye leakage to the contralateral hemicord.

Figure 7 Continued
maximum in the lumbar segment and lowest in the cervical cord. (**M–P**) Schematic illustrating the likely pathway of dye transport through propriospinal interneurons in the thoraco-lumbar and thoracic spinal segments. The number of labelled cells is similar in **N** and **M** and suggests an underlying mechanism of neuronal organization, i.e. axonal sprouting or activation of dormant neurons (dotted coloured lines) that are likely responsible for the higher neuronal count observed after quadrupedal step-training. (**Q**) Conceptual model for the observed results: schematic illustrating neuronal pathways that may be modulated by quadrupedal step-training. Afferent input from the forelimbs activates the lumbosacral locomotor networks (LLN) in the spinal cord through direct activation of (**i**) long (solid long arrow); and/or (**ii**) intersegmental short propriospinal neurons (solid short arrows); (**iii**) a longer neuronal loop (spino-bulbo-spinal pathways) that projects from the forelimbs to the brain and eventually down to the lumbosacral locomotor network; (**iv**) a bulbospinal direct relay that activates the lumbosacral locomotor network; and/or (**v**) descending supraspinal pathways that activate the propriospinal system (red dotted arrows).

In contrast to the absence of labelled cells in the long descending cervical propriospinal neurons, large numbers of short propriospinal neurons were labelled bilaterally in all animals in the thoracic and lumbar segments, above and below the lesion site. These findings are consistent with a previous report showing retrogradely labelled short propriospinal neurons bilaterally above and below a lateral thoracic hemisection lesion in mice allowed to recover spontaneously (Courtine *et al*., 2009). These short neurons may create new functional circuits around an incomplete lesion and provide the substrate for locomotor recovery.

Based on the present results, we propose that training the forelimbs significantly impacted the hindlimbs through a link of intersegmental connecting interneurons. As such, the propriospinal axons from the cervical cord segmentally activate interneurons in the thoracic segments that, in turn, activate neurons in the lumbar segments [Fig. 7Q(ii)], a hypothesis previously suggested in the cat (Aoki and McIntyre, 1975; Shik, 1997; Manjarrez *et al*., 2003) and neonatal rat (Juvin *et al*., 2005; Cowley *et al*., 2008). Studies in the neonatal rat demonstrate that the propriospinal relay system serves as an important and likely sufficient conduit for descending activation of the locomotor networks (Cowley *et al*., 2008). Indeed, a drastic reduction in locomotor cervico-lumbar coordination is observed when the excitability of thoracic neural elements is decreased or when synaptic transmission in these segments is suppressed (Juvin *et al*., 2005, 2012). Additionally, the short propriospinal neurons primarily located in T6–T8 which innervate lumbar motor neuronal pools (Conta and Stelzner, 2004) may also relay signals from the long supraspinal descending systems to the motor neurons in the lumbar cord, as shown in the cat (Vasilenko *et al*., 1972). In fact, based on the latency of the evoked responses from the triceps brachii muscle in response to magnetic stimulation of the sciatic nerve (Beaumont *et al*., 2006), it was suggested that transmission through this ascending propriospinal pathway likely involves three to five synapses, providing further evidence of extant polysynaptic connections between the forelimbs and hindlimbs. Reorganization of the thoraco-lumbar spinal circuitry by sprouting of spared fibres (Siebert *et al*., 2010; Darlot *et al*., 2012) and/or alterations in the strength of existing neural circuits through, e.g. changes in neurotransmitter release or postsynaptic receptor density (Flynn *et al*., 2011), may account for the increased number of labelled cells observed after quadrupedal step-training. Alternatively, the possibility exists that propriospinal axons engaged in more activity (as a result of forced forelimb training) took up and transported the retrograde tracer more efficiently, resulting in the differences in labelling among groups.

The greater number of labelled cells in the thoracic segments of quadrupedal step-trained rats represents increased excitation of thoracic interneurons through rostrally connecting interneurons. The remarkable improvements in locomotor function and bilateral symmetry in the excitability of lumbosacral motor neurons in quadrupedal step-trained rats also suggests that these neurons were responsive to the training paradigm. Given that the propriospinal system is implicated in the regulation of the axial musculature and in postural mechanisms (Anderson, 1963; Vasilenko, 1975), it is very likely that the trunk afferents and musculature that are rhythmically active during locomotion (Giszter *et al*., 2008) exert greater control over the hindlimb musculature after quadrupedal step-training than bipedal step-training for effective quadrupedal locomotion. After quadrupedal step-training, the rats step effectively without tail support unlike bipedal step-trained and non-trained rats (Supplementary Video 1). As such, we suggest that the anatomical reorganization of the thoracic interneurons contributed to improved postural control of the trunk, and hence hindlimb locomotion. Interestingly, our results show that the vertical distance between the pelvis/knee to the ground (indicating vertical postural alignment) is similar between the trained groups and pre-hemisection (Supplementary Fig. 2C and D). Collectively, these data suggest that improvements in gross adaptive postural control of the trunk (Giszter *et al*., 2008) might partially contribute to enhanced locomotor function, but is not a major contributor in the differential recovery observed 'among' groups.

In conclusion, hindlimb function and coordination patterns improve after a hemisection when the locomotor circuitry is activated, presumably as a result of neuromodulation via sensory input from the forelimbs. The propriospinal system strategically integrates signals from supraspinal (and spinal) centres with those from the periphery for accurate activation of motor neuronal pools (Darlot *et al*., 2012; van den Brand *et al*., 2012). Based on the present data alone, we cannot distinguish to what extent the improved motor function observed is attributable to the reorganization of supraspinal descending pathways [Fig. 7Q(iv-v)] versus changes in the processing of sensory input (proprioception and cutaneous) to the propriospinal pathways [Fig. 7Q(i–iii)].

Relevance to clinical rehabilitation

Observations of the impact of upper extremity training on lower extremity function in persons with spinal cord injury are preliminary and inconclusive. We demonstrate that actively engaging the forelimbs when training the hindlimbs in hemisection rats can enhance hindlimb locomotor function to a much greater extent than with hindlimb training alone. Identification of this phenomenon provides a strong rationale for proceeding toward preclinical studies for determining whether training paradigms involving active upper arm training in concert with lower extremity training can enhance locomotor recovery after neurological damage. Examples of such training paradigms might include arm-cycling during functional electrical stimulation leg-cycling exercises, use of an elliptical trainer after incomplete paraparesis, and active arm-swinging during overground locomotion and treadmill training.

Funding

This work is supported by the Craig Neilsen Foundation Post-Doctoral Fellowship award granted to PKS (Grant # 82616); Christopher and Dana Reeve Foundation; the programs Number 5 and 7 of the Presidium of RAN; the Russian Foundation of Basic Research Grants: 13-04-01091 and 13-04-12030-ofi_m; and the National Institute of Biomedical Imaging and Bioengineering R01EB007615.

Supplementary material

Supplementary material is available at *Brain* online.

References

Akay T, McVea DA, Tachibana A, Pearson KG. Coordination of fore and hind leg stepping in cats on a transversely-split treadmill. Exp Brain Res 2006; 175: 211–22.

Anderson FD. The structure of a chronically isolated segment of the cat spinal cord. J Comp Neurol 1963; 120: 297–315.

Aoki M, McIntyre AK. Cortical and long spinal actions on lumbosacral motoneurones in the cat. J Physiol 1975; 251: 569–87.

Ballermann M, Fouad K. Spontaneous locomotor recovery in spinal cord injured rats is accompanied by anatomical plasticity of reticulospinal fibers. Eur J Neurosci 2006; 23: 1988–96.

Bareyre FM, Kerschensteiner M, Raineteau O, Mettenleiter TC, Weinmann O, Schwab ME. The injured spinal cord spontaneously forms a new intraspinal circuit in adult rats. Nat Neurosci 2004; 7: 269–77.

Battistuzzo CR, Callister RJ, Callister R, Galea MP. A systematic review of exercise training to promote locomotor recovery in animal models of spinal cord injury. J Neurotrauma 2012; 29: 1600–13.

Beaumont E, Onifer SM, Reed WR, Magnuson DS. Magnetically evoked inter-enlargement response: an assessment of ascending propriospinal fibers following spinal cord injury. Exp Neurol 2006; 201: 428–40.

Behrman AL, Harkema SJ. Locomotor training after human spinal cord injury: a series of case studies. Phys Ther 2000; 80: 688–700.

Conta AC, Stelzner DJ. Differential vulnerability of propriospinal tract neurons to spinal cord contusion injury. J Comp Neurol 2004; 479: 347–59.

Conta AC, Stelzner DJ. Loss of propriospinal neurons after spinal contusion injury as assessed by retrograde labeling. Neuroscience 2010; 170: 971–80.

Courtine G, Gerasimenko Y, van den Brand R, Yew A, Musienko P, Zhong H, et al. Transformation of nonfunctional spinal circuits into functional states after the loss of brain input. Nat Neurosci 2009; 12: 1333–42.

Cowley KC, Zaporozhets E, Schmidt BJ. Propriospinal neurons are sufficient for bulbospinal transmission of the locomotor command signal in the neonatal rat spinal cord. J Physiol 2008; 586: 1623–35.

Darlot F, Cayetanot F, Gauthier P, Matarazzo V, Kastner A. Extensive respiratory plasticity after cervical spinal cord injury in rats: axonal sprouting and rerouting of ventrolateral bulbospinal pathways. Exp Neurol 2012; 236: 88–102.

Deng LX, Deng P, Ruan Y, Xu ZC, Liu NK, Wen X, et al. A novel growth-promoting pathway formed by GDNF-overexpressing schwann cells promotes propriospinal axonal regeneration, synapse formation, and partial recovery of function after spinal cord injury. J Neurosci 2013; 33: 5655–67.

Dietz V, Michel J. Human bipeds use quadrupedal coordination during locomotion. Ann N Y Acad Sci 2009; 1164: 97–103.

Efron B, Tibshirani R. Statistical data analysis in the computer age. Science 1991; 253: 390–5.

Ferris DP, Huang HJ, Kao PC. Moving the arms to activate the legs. Exerc Sport Sci Rev 2006; 34: 113–20.

Flynn JR, Graham BA, Galea MP, Callister RJ. The role of propriospinal interneurons in recovery from spinal cord injury. Neuropharmacology 2011; 60: 809–22.

Gerasimenko Y, Musienko P, Bogacheva I, Moshonkina T, Savochin A, Lavrov I, et al. Propriospinal bypass of the serotonergic system that can facilitate stepping. J Neurosci 2009; 29: 5681–9.

Giszter S, Davies MR, Ramakrishnan A, Udoekwere UI, Kargo WJ. Trunk sensorimotor cortex is essential for autonomous weight-supported locomotion in adult rats spinalized as P1/P2 neonates. J Neurophysiol 2008; 100: 839–51.

Houle JD, Tom VJ, Mayes D, Wagoner G, Phillips N, Silver J. Combining an autologous peripheral nervous system "bridge" and matrix modification by chondroitinase allows robust, functional regeneration beyond a hemisection lesion of the adult rat spinal cord. J Neurosci 2006; 26: 7405–15.

Huang HJ, Ferris DP. Neural coupling between upper and lower limbs during recumbent stepping. J Appl Physiol 2004; 97: 1299–308.

Hundza SR, Zehr EP. Suppression of soleus H-reflex amplitude is graded with frequency of rhythmic arm cycling. Exp Brain Res 2009; 193: 297–306.

Iannotti C, Li H, Yan P, Lu X, Wirthlin L, Xu XM. Glial cell line-derived neurotrophic factor-enriched bridging transplants promote propriospinal axonal regeneration and enhance myelination after spinal cord injury. Exp Neurol 2003; 183: 379–93.

Jankowska E, Hammar I, Chojnicka B, Heden CH. Effects of monoamines on interneurons in four spinal reflex pathways from group I and/or group II muscle afferents. Eur J Neurosci 2000; 12: 701–14.

Jankowska E, Lundberg A, Roberts WJ, Stuart D. A long propriospinal system with direct effect on motoneurones and on interneurones in the cat lumbosacral cord. Exp Brain Res 1974; 21: 169–94.

Juvin L, Le Gal JP, Simmers J, Morin D. Cervicolumbar coordination in mammalian quadrupedal locomotion: role of spinal thoracic circuitry and limb sensory inputs. J Neurosci 2012; 32: 953–65.

Juvin L, Simmers J, Morin D. Propriospinal circuitry underlying interlimb coordination in mammalian quadrupedal locomotion. J Neurosci 2005; 25: 6025–35.

Kausz M. Distribution of neurons in the lateral pontine tegmentum projecting to thoracic, lumbar and sacral spinal segments in the cat. J Hirnforsch 1986; 27: 485–93.

Kawashima N, Nozaki D, Abe MO, Nakazawa K. Shaping appropriate locomotive motor output through interlimb neural pathway within spinal cord in humans. J Neurophysiol 2008; 99: 2946–55.

Kazennikov OV, Beliaev KR, Iakovleva GV, Shik ML. Synaptic responses of spinal cord neurons to rhythmic microstimulation of a stepping strip [in Russian]. Neirofiziologiia 1991; 23: 631–3.

Kostyuk PG, Vasilenko DA. Spinal interneurons. Annu Rev Physiol 1979; 41: 115–26.

Lavrov I, Gerasimenko YP, Ichiyama RM, Courtine G, Zhong H, Roy RR, et al. Plasticity of spinal cord reflexes after a complete transection in adult rats: relationship to stepping ability. J Neurophysiol 2006; 96: 1699–710.

Lopez-Dolado E, Lucas-Osma AM, Collazos-Castro JE. Dynamic motor compensations with permanent, focal loss of forelimb force after cervical spinal cord injury. J Neurotrauma 2013; 30: 191–210.

Manjarrez E, Jimenez I, Rudomin P. Intersegmental synchronization of spontaneous activity of dorsal horn neurons in the cat spinal cord. Exp Brain Res 2003; 148: 401–13.

Mezzarane RA, Klimstra M, Lewis A, Hundza SR, Zehr EP. Interlimb coupling from the arms to legs is differentially specified for populations of motor units comprising the compound H-reflex during "reduced" human locomotion. Exp Brain Res 2011; 208: 157–68.

National Research Council. Guide for the care and use of laboratory animals. Washington, DC: National Academy Press; 2011.

Perennou D. Physiology and pathophysiology of postural control. Lett Phys Readapt Med 2012; 28: 120–32.

Reed WR, Shum-Siu A, Onifer SM, Magnuson DS. Inter-enlargement pathways in the ventrolateral funiculus of the adult rat spinal cord. Neuroscience 2006; 142: 1195–207.

Reed WR, Shum-Siu A, Whelan A, Onifer SM, Magnuson DS. Anterograde labeling of ventrolateral funiculus pathways with spinal enlargement connections in the adult rat spinal cord. Brain Res 2009; 1302: 76–84.

Roy RR, Hutchison DL, Pierotti DJ, Hodgson JA, Edgerton VR. EMG patterns of rat ankle extensors and flexors during treadmill locomotion and swimming. J Appl Physiol 1991; 70: 2522–9.

Schomburg ED, Steffens H. Synaptic responses of lumbar alpha-motoneurones to selective stimulation of cutaneous nociceptors and low

threshold mechanoreceptors in the spinal cat. Exp Brain Res 1986; 62: 335–42.
Shah PK, Gerasimenko Y, Shyu A, Lavrov I, Zhong H, Roy RR, et al. Variability in step training enhances locomotor recovery after a spinal cord injury. Eur J Neurosci 2012; 36: 2054–62.
Shah PK, Song J, Kim S, Zhong H, Roy RR, Edgerton VR. Rodent estrous cycle response to incomplete spinal cord injury, surgical interventions, and locomotor training. Behav Neurosci 2011; 125: 996–1002.
Shik ML. Recognizing propriospinal and reticulospinal systems of initiations of stepping. Motor Control 1997; 1: 310–3.
Shimamura M, Mori S, Yamauchi T. Effects of spino-bulbo-spinal reflex volleys on extensor motoneurons of hindlimb in cats. J Neurophysiol 1967; 30: 319–32.
Siebert JR, Middleton FA, Stelzner DJ. Long descending cervical propriospinal neurons differ from thoracic propriospinal neurons in response to low thoracic spinal injury. BMC Neurosci 2010; 11: 148.
Tester NJ, Howland DR, Day KV, Suter SP, Cantrell A, Behrman AL. Device use, locomotor training and the presence of arm swing during treadmill walking after spinal cord injury. Spinal Cord 2011; 49: 451–6.
van den Brand R, Heutschi J, Barraud Q, DiGiovanna J, Bartholdi K, Huerlimann M, et al. Restoring voluntary control of locomotion after paralyzing spinal cord injury. Science 2012; 336: 1182–5.
Vasilenko DA. Propriospinal pathways in the ventral funicles of the cat spinal cord: their effects on lumbosacral motoneurones. Brain Res 1975; 93: 502–6.
Vasilenko DA, Kostiukov AI, Piliavskii AI. Cortico-and rubrofugal activation of interneurons forming the propriospinal tracts of the dorsolateral funiculus of the cat spinal cord [in Russian]. Neirofiziologiia 1972; 4: 489–500.
Visintin M, Barbeau H. The effects of parallel bars, body weight support and speed on the modulation of the locomotor pattern of spastic paretic gait. A preliminary communication. Paraplegia 1994; 32: 540–53.
Watson C PG, Kayalioglu G. Atlas of the rat spinal cord. London: Elsivier; 2009.
Zehr EP, Duysens J. Regulation of arm and leg movement during human locomotion. Neuroscientist 2004; 10: 347–61.
Zehr EP, Klimstra M, Dragert K, Barzi Y, Bowden MG, Javan B, et al. Enhancement of arm and leg locomotor coupling with augmented cutaneous feedback from the hand. J Neurophysiol 2007; 98: 1810–4.